

Published in final edited form as:

Chem Commun (Camb). 2014 June 7; 50(45): 6039–6042. doi:10.1039/c3cc49453e.

Linker-Determined Drug Release Mechanism of Free Camptothecin from Self-Assembling Drug Amphiphiles†

Andrew G. Cheetham, Yu-Chuan Ou, Pengcheng Zhang, and Honggang Cui

Department of Chemical and Biomolecular Engineering and Institute for BioNanoTechnology (INBT), The Johns Hopkins University, Baltimore, MD 21218, USA

Honggang Cui: hcui6@jhu.edu

Abstract

We report here that the release mechanism of free camptothecin from self-assembling drug amphiphiles can be regulated by use of different linker groups. Our results highlight the significance of the linker group of drug amphiphiles on the drug release efficiency and their consequent *in vitro* efficacy.

Covalent linkage of anticancer drugs to a carrier presents an effective strategy to improve the drug's solubility, to enhance the drug targeting efficiency,¹ and to help circumvent multidrug resistance.² Such a prodrug strategy has been used to create peptide–drug conjugates,³ polymer–drug conjugates,⁴ dendrimer–drug conjugates,⁵ nanoparticle–drug conjugates,⁶ and most recently drug-based molecular hydrogelators⁷ and self-assembling drug amphiphiles.⁸ Indeed, the linkage of a hydrophilic segment to a hydrophobic anticancer drug to create self-assembling amphiphiles offers the means to create self-delivering drugs that possess a high and fixed drug content, allowing for the minimum use of excipients. These self-assembling prodrugs combine the processability of small molecules with the controlled pharmacokinetics potential offered by larger structures such as polymer–drug conjugates.^{4b, 9} One characteristic that all these drug conjugates must share is the ability to effectively release their cargo in an active form at the target site. A popular method for this is the use of stimuli-sensitive linkers¹⁰ between the drug and carrier that can selectively release the drug, examples of which include pH-,¹¹ reduction-,^{2, 12} or enzyme-sensitive¹³ linkers. The linker is thus of critical importance in determining the overall efficacy of the delivery system and, at times can be complicated by the auxiliary segment^{5b, 14} and also by drug's chemical structure. For example, work by Low and co-workers¹² reveals that a camptothecin (CPT)–folate conjugate with a disulfanyl butyrate linker shows lower activity against cancer cell lines in comparison to its carbonate analogue, and attributed this to the lack of endosomal esterases that can accelerate hydrolysis of the cleaved thiol. In contrast, a report by Wender and co-workers suggests that intramolecular cyclization of the cleaved thiol to form a 5-membered lactone can help spur the release of the free drug in paclitaxel (PTX)-conjugated octaarginine transporters,² with this conjugate showing greater activity

Electronic Supplementary Information (ESI) available: Experimental methods, characterization data. See DOI: 10.1039/c000000x/

© The Royal Society of Chemistry 2012

Correspondence to: Honggang Cui, hcui6@jhu.edu.

than its carbonate analogue. These contradictory results may be due to greater steric hindrance around the 3° hydroxyl of CPT versus the 2° hydroxyl of PTX.

We recently reported the creation of drug amphiphiles (DAs)—peptide–drug conjugates with the capacity for self-assembly into well-defined nanostructures.⁸ Our initial design^{8a} connected the hydrophobic anticancer drug camptothecin¹⁵ to a hydrophilic β -sheet forming Tau-derived peptide¹⁶ via a reducible disulfanyl butyrate (buSS) linker. The single CPT-containing buSS-linked drug amphiphile displayed a much reduced activity when compared with free CPT, an observation that may be due to the release of the active drug. In this communication, we show that the *in vitro* activity of this buSS-linked drug amphiphile is compromised by the nanostructure-promoted formation and protection of a CPT-based disulphide dimer that reduces its ability to release the free drug (Fig. 1). The carbonate-based analogue, which undergoes rapid self-immolation upon reduction, was found to largely negate this effect.

To probe the release of CPT from the buSS-linked drug amphiphile, **CPT-buSS-Tau (1)**,^{8a} we performed a more mechanistic study of its glutathione (GSH)-induced degradation using HPLC and LC-MS analyses at relatively low (5 μ M) and high (50 μ M) concentrations. This allows us to explore the degradation behaviour close to and much higher than the critical assembly concentration, which was previously found to be sub-micromolar.^{8a} Following the initial reduction of the buSS linker, a dynamic mixture of products is expected to form through a series of disulphide exchange and hydrolysis reactions (Fig. 2a). It can be seen from the HPLC analysis that reduction of **1** proceeded to give free CPT via two intermediary species at 11.7 and 15.7 min (Fig. 2b–c). LC-MS analysis (S3.3 and Fig. S11 in ESI†) identified the first of these as the expected cleavage product, **3**, with the second being the symmetrical CPT-containing disulphide dimer, **4**. To the best of our knowledge, this is the first time that such a disulphide species has been reported to have been formed through reduction of this linker type. The efficiency with which free CPT is released is therefore dependent upon the stability of these two intermediates.

Examining the release profile over a 24 h period shows that the solution concentration has a significant effect on the amount of released CPT (Fig. 2d–e). At low concentrations, **3** and **4** make up around 13% of the total CPT-containing components in solution after 24 h, with approximately 49% free CPT released. In contrast, **3** and **4** make up 34% after 24 h at the 50 μ M concentration with only 26% free CPT released. This occurs despite a similar level of degradation of the parent conjugate **1** (almost 60% loss at both concentrations). The data also show that at the higher concentration, **4** appears to undergo little further hydrolysis or reduction, even increasing slightly, after 7 h incubation, whereas **3** depletes at both concentrations. This clearly indicates that there is some stabilizing influence over the disulphide dimer that prevents further degradation at the higher concentration. There is also little evidence to suggest that the degradation of **3** is undergoing any accelerated release due to intramolecular cyclization, instead being simply hydrolysed in agreement with the observations of Low and co-workers.¹²

A comparison of the GSH-induced CPT release from solutions of DA **1** and the non-assembling **CPT-buSS-Pyr** conjugate (both 25 μ M) found that reduction of **1** generates

twice the relative amount of **4** than **CPT-buSS-Pyr** (Fig. S12 in ESI[†]). Interestingly, this experiment also shows that **CPT-buSS-GSH** is very sensitive to further degradation as a significant amount of free CPT has already been generated after only 1 h of incubation. This observation suggests that in the early stages of reaction, the reduction of DA **1** proceeds predominantly via the formation of sulphide **3** and **Tau-GSH** (as identified by LC-MS analysis, Fig. S11g in ESI[†]), because there is little evidence of **CPT-buSS-GSH** and only a small amount of CPT formed within 1 h. The released **3** would then go on to form the disulphide dimer by further reaction with **1**. It is clear from these results that the supramolecular nature of the conjugate is affecting the release process.

Taking into account the supramolecular nature of DA **1**,^{8a} the data obtained suggests the mechanism shown in Fig. 2f as a possible explanation for the observed disulphide formation and subsequent stability. In a fully assembled state, the disulphide bond of **1** will only be able to react with GSH at the terminal ends of the nanofilaments or, more likely, with those in smaller β -sheet aggregates that have dissociated from the larger nanostructures. The close proximity of the newly released **3** (as the thiolate) to a neighbouring conjugate molecule would then make disulphide exchange highly favourable, either reforming **1** or giving the disulphide dimer **4**. This reaction of GSH with nanofibers or non-micellar β -sheet structures is expected to be enhanced at relatively higher concentrations, accounting for the greater fraction of **4** at 50 μ M relative to that of 5 μ M. Since the CPT segment is hydrophobic and possesses the potential for π - π interactions, molecules of **4** formed from reaction of GSH with nanofilaments or non-micellar β -sheets at higher concentrations may remain associated with the larger nanostructure or form some other types of aggregates, rather than escaping into the aqueous environment. As a result these disulphide dimers would be protected from hydrolysis that would give free CPT. At low concentrations, the degradation of the conjugate will lead to eventual disassembly of the nanofibers or β -sheets as the concentration falls closer to the critical aggregation concentration with subsequent exposure of the CPT-products to water—the significant proportion of **4** remaining after 24 h incubation at 50 μ M in comparison to the 5 μ M study is in agreement with this proposition.

To negate the effect of this nanostructure-promoted disulphide formation, we incorporated a carbonate-based linker that has a greater propensity for self-immolation. Our rationale is that if the release product can rapidly degrade then it should reduce any opportunity for disulphide formation. To this end, we utilized the disulfanyl-ethyl carbonate linker^{2, 12, 17} to furnish **CPT-etcSS-Tau, 2** (Fig. 1 and Scheme S2 in ESI[†]). It has been proposed that, upon reduction, this linker can release the attached cargo via a two-step pathway to produce the free drug (Fig. 3a), with thiolate **5** undergoing intramolecular displacement to give carbonate **6**, which then decarboxylates to give free CPT.¹⁷ The observation of the rapid hydrolysis of peptide thioesters in the presence of 2-mercaptoethanol provides validation for this intramolecular displacement step.¹⁸

Self-assembly of **2** was seen to give similar filamentous nanostructures to **1** (Fig. 1), with CD analysis confirming the β -sheet structure was present (Fig. S9 in ESI[†]). Given that the nature of the linker has no significant effect on the nanostructure adopted, the drug release was studied using the same protocol. We found that the GSH-induced cleavage of **2** occurs very rapidly (Fig. 3b–c), generating only the free drug. A room temperature study confirmed

no appreciable amount of intermediates **5** and **6** were formed (Fig. 3b), indicating that rapid degradation via the expected intramolecular pathway was occurring rather than direct hydrolysis at the elevated temperature. A kinetic study also confirmed that the conjugate possesses excellent hydrolytic stability (Fig. 3c). It is clear that the fast and direct conversion to free CPT upon GSH reduction of **2** eliminates any possibility of disulphide formation due to the self-assembled nature of the conjugate.

In vitro experiments using the MCF-7 breast cancer cell line were performed to determine the relative cytotoxicity of DAs **1** and **2**, and their degradation products **3**, **4** and ethylene sulphide (Fig. 4). It can be seen that the carbonate linker of **2** offers a greater efficacy compared to the ester linker of **1**, being comparable to free CPT. This result is consistent with previous observations¹² and our release experiments. Interestingly, intermediate **3** was found to have a similar toxicity to free CPT, whereas disulphide **4** was comparable to its parent DA, **1**. That **3** is apparently more toxic than both **1** and **4** may be due its greater susceptibility to hydrolysis (less propensity for aggregation) and differences in cellular uptake. The proposed release product from the degradation of **2**, ethylene sulphide, was found to be non-toxic over the studied range, indicating the toxicity of **2** arises solely from the release of CPT.

In summary, our studies have revealed that the filamentous nature of disulfanyl ester-linked CPT drug amphiphiles can promote the formation of CPT-based disulphide dimers upon reduction, with higher concentrations of the conjugate reducing the amount of bioactive CPT being released through apparent protection of the intermediates from hydrolysis. Incorporating a carbonate-based linker restored much of the conjugated drug's activity by facilitating a more effective release upon reduction, giving a more potent drug amphiphile.

Supplementary Material

Refer to Web version on PubMed Central for supplementary material.

Acknowledgments

This work was supported by the National Science Foundation (DMR 1255281) and NIH (A.C.: T-32CA130840). We acknowledge the use of the JHU Department of Chemistry Shared Facilities and the Integrated Imaging Center (IIC).

Notes and references

1. (a) Arap W, Pasqualini R, Ruoslahti E. *Science*. 1998; 279:377–380. [PubMed: 9430587] (b) Sievers EL, Linenberger M. *Curr. Opin. Oncol.* 2001; 13:522–527. [PubMed: 11673694]
2. Dubikovskaya EA, Thorne SH, Pillow TH, Contag CH, Wender PA. *Proc. Natl. Acad. Sci. U. S. A.* 2008; 105:12128–12133. [PubMed: 18713866]
3. Ahrens VM, Bellmann-Sickert K, Beck-Sickinger AG. *Future Med. Chem.* 2012; 4:1567–1586. [PubMed: 22917246]
4. (a) McDaniel JR, Bhattacharyya J, Vargo KB, Hassouneh W, Hammer DA, Chilkoti A. *Angew. Chem., Int. Ed.* 2013; 52:1683–1687. (b) Duncan R. *Nat. Rev. Cancer.* 2006; 6:688–701. [PubMed: 16900224] (c) Tong R, Cheng J. *Macromolecules.* 2012; 45:2225–2232. [PubMed: 23357880] (d) Zou J, Jafr G, Themistou E, Yap Y, Wintrob ZAP, Alexandridis P, Ceacareanu AC, Cheng C. *Chem. Commun.* 2011; 47:4493–4495. (e) Tong R, Cheng J. *J. Am. Chem. Soc.* 2009; 131:4744–4754. [PubMed: 19281160]

5. (a) Sunoqrot S, Liu Y, Kim D-H, Hong S. *Mol. Pharm.* 2012; 10:2157–2166. [PubMed: 23234605]
(b) Kurtoglu YE, Mishra MK, Kannan S, Kannan RM. *Int. J. Pharm.* 2010; 384:189–194. [PubMed: 19825406]
6. Vigderman L, Zubarev ER. *Adv. Drug Delivery Rev.* 2013; 65:663–676.
7. (a) Gao Y, Kuang Y, Guo ZF, Guo ZH, Krauss IJ, Xu B. *J. Am. Chem. Soc.* 2009; 131:13576–13577. [PubMed: 19731909] (b) Yang C, Li D, Feng Zhao Q, Wang L, Wang L, Yang Z. *Org. Biomol. Chem.* 2013; 49:6946–6951. [PubMed: 23989242]
8. (a) Cheetham AG, Zhang P, Lin Y-A, Lock LL, Cui H. *J. Am. Chem. Soc.* 2013; 135:2907–2910. [PubMed: 23379791] (b) Lin R, Cheetham AG, Zhang P, Lin YA, Cui H. *Chem. Commun.* 2013; 49:4968–4970.
9. Tong R, Cheng J. *Polym. Rev.* 2007; 47:345–381.
10. D'Souza AJM, Topp EM. *J. Pharm. Sci.* 2004; 93:1962–1979. [PubMed: 15236447]
11. Furgeson DY, Dreher MR, Chilkoti A. *J. Controlled Release.* 2006; 110:362–369.
12. Henne WA, Doorneweerd DD, Hilgenbrink AR, Kularatne SA, Low PS. *Bioorg. Med. Chem. Lett.* 2006; 16:5350–5355. [PubMed: 16901694]
13. Gabriel D, Zuluaga MF, van den Bergh H, Gurny R, Lange N. *Curr. Med. Chem.* 2011; 18:1785–1805. [PubMed: 21466472]
14. Penugonda S, Kumar A, Agarwal HK, Parang K, Mehvar R. *J. Pharm. Sci.* 2008; 97:2649–2664. [PubMed: 17853426]
15. Pommier Y. *Nat. Rev. Cancer.* 2006; 6:789–802. [PubMed: 16990856]
16. Goux WJ, Kopplin L, Nguyen AD, Leak K, Rutkofsky M, Shanmuganandam VD, Sharma D, Inouye H, Kirschner DA. *J. Biol. Chem.* 2004; 279:26868–26875. [PubMed: 15100221]
17. Kularatne SA, Venkatesh C, Santhapuram H-KR, Wang K, Vaitilingam B, Henne WA, Low PS. *J. Med. Chem.* 2010; 53:7767–7777. [PubMed: 20936874]
18. Gates ZP, Stephan JR, Lee DJ, Kent SBH. *Chem. Commun.* 2013; 49:786–788.

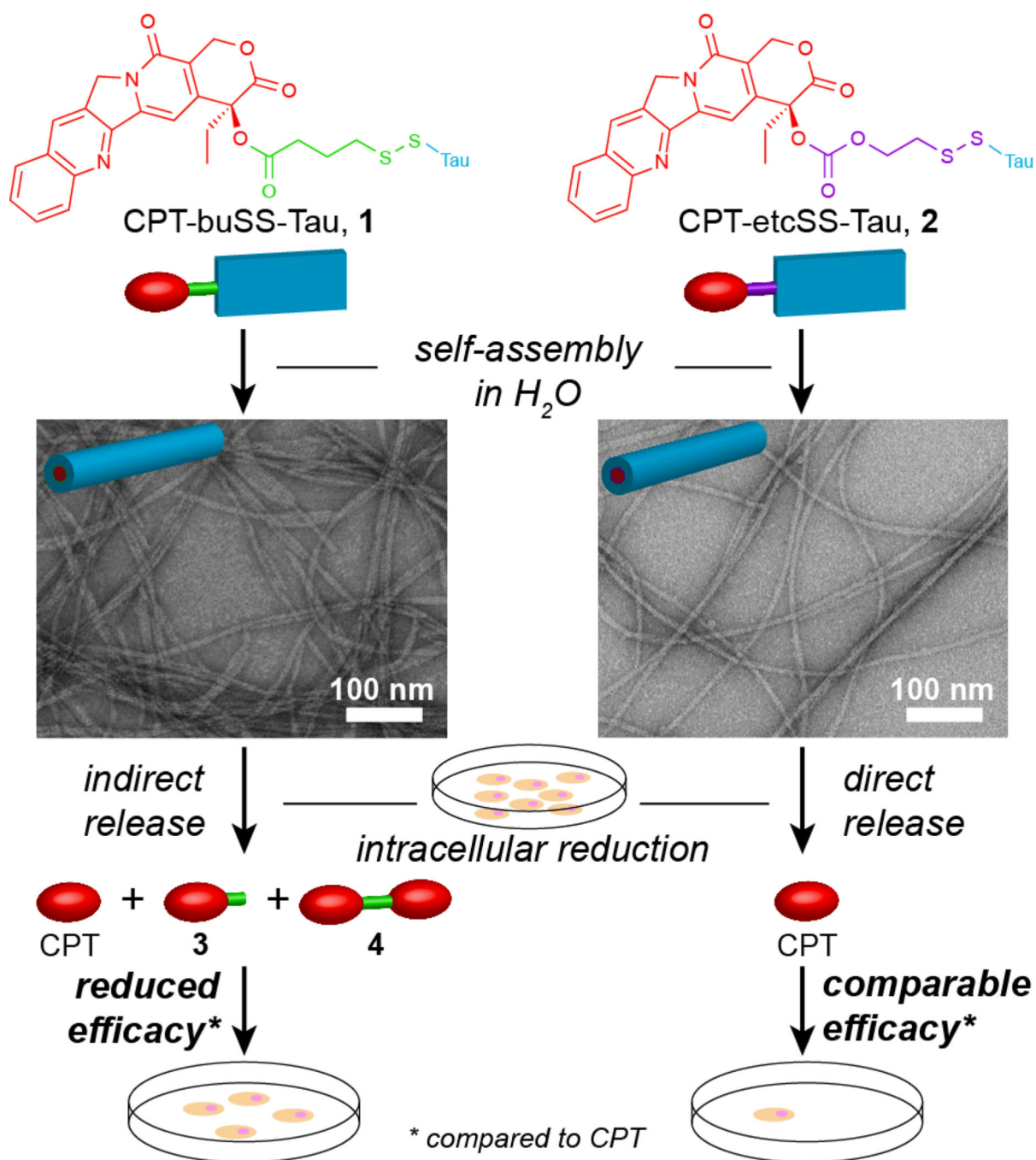


Fig. 1. Self-assembly of the ester-based **CPT-buSS-Tau (1)** and carbonate-based **CPT-etcSS-Tau (2)** drug amphiphiles into nanofilamentous structures and the effect of the linker on the release mechanism of the free drug, CPT, and the subsequent cytotoxicity. Representative TEM images were obtained from 1 mM samples of **1** and **2** in water, staining with 2 wt % uranyl acetate.

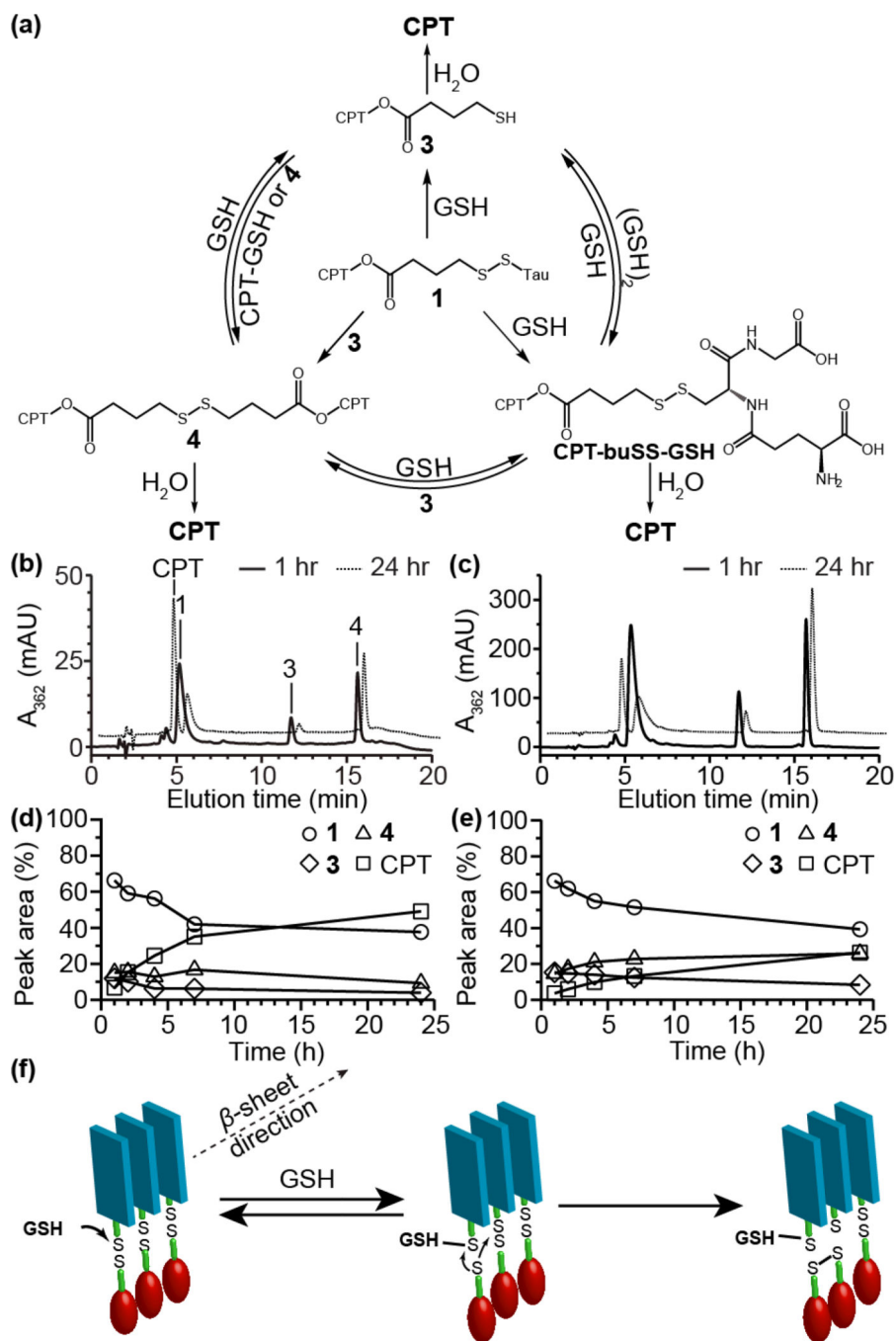
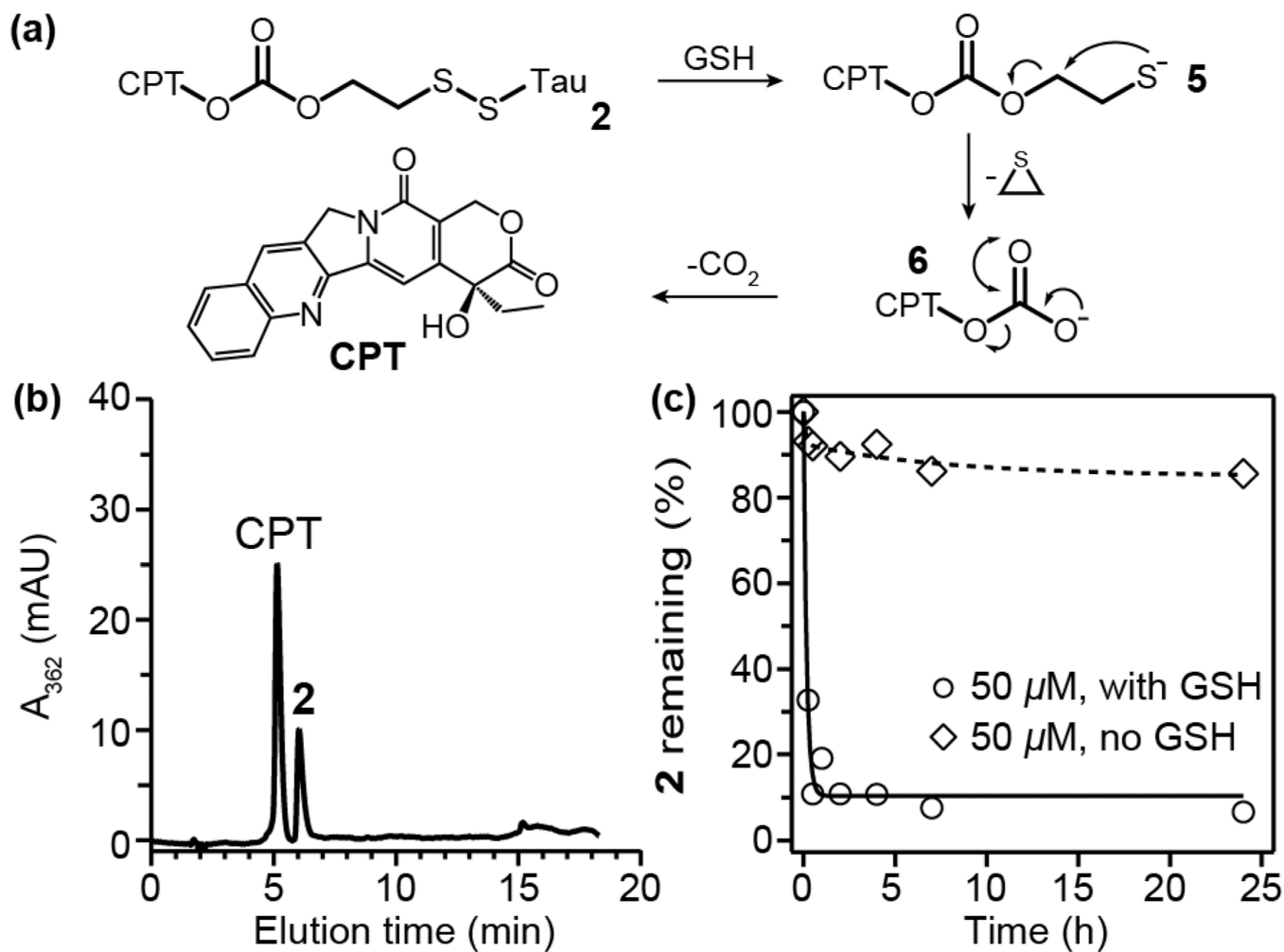


Fig. 2. GSH-induced release of CPT from **1**. CPT-containing reaction products formed and the exchange reactions that can occur during the GSH-induced reduction of **1** (a). HPLC analysis of GSH-induced release of CPT from DA **1** at 5 (b) and 50 μM (c) in 10 mM sodium phosphate containing 10 mM GSH at 37 $^{\circ}\text{C}$ after 1 and 24 h. Peak areas of the 4 main species (expressed as percentages of the total area; the area for **4** was halved to reflect the increased absorbance due to two CPT molecules) showing the evolution over time for

the 5 (d) and 50 μM (e) solutions of **1**. Possible mechanism for the formation of the disulphide dimer **4** within nanofilaments or smaller β -sheet aggregates (f).

**Fig. 3.**

(a) Mechanism of GSH induced release from **2**. (b) HPLC analysis of a solution with **2** (50 μM) and 10 mM GSH in 10 mM sodium phosphate after 50 min at room temperature. (c) Degradation of **2** (50 μM) with or without 10 mM GSH in 10 mM sodium phosphate at 37 $^{\circ}\text{C}$.

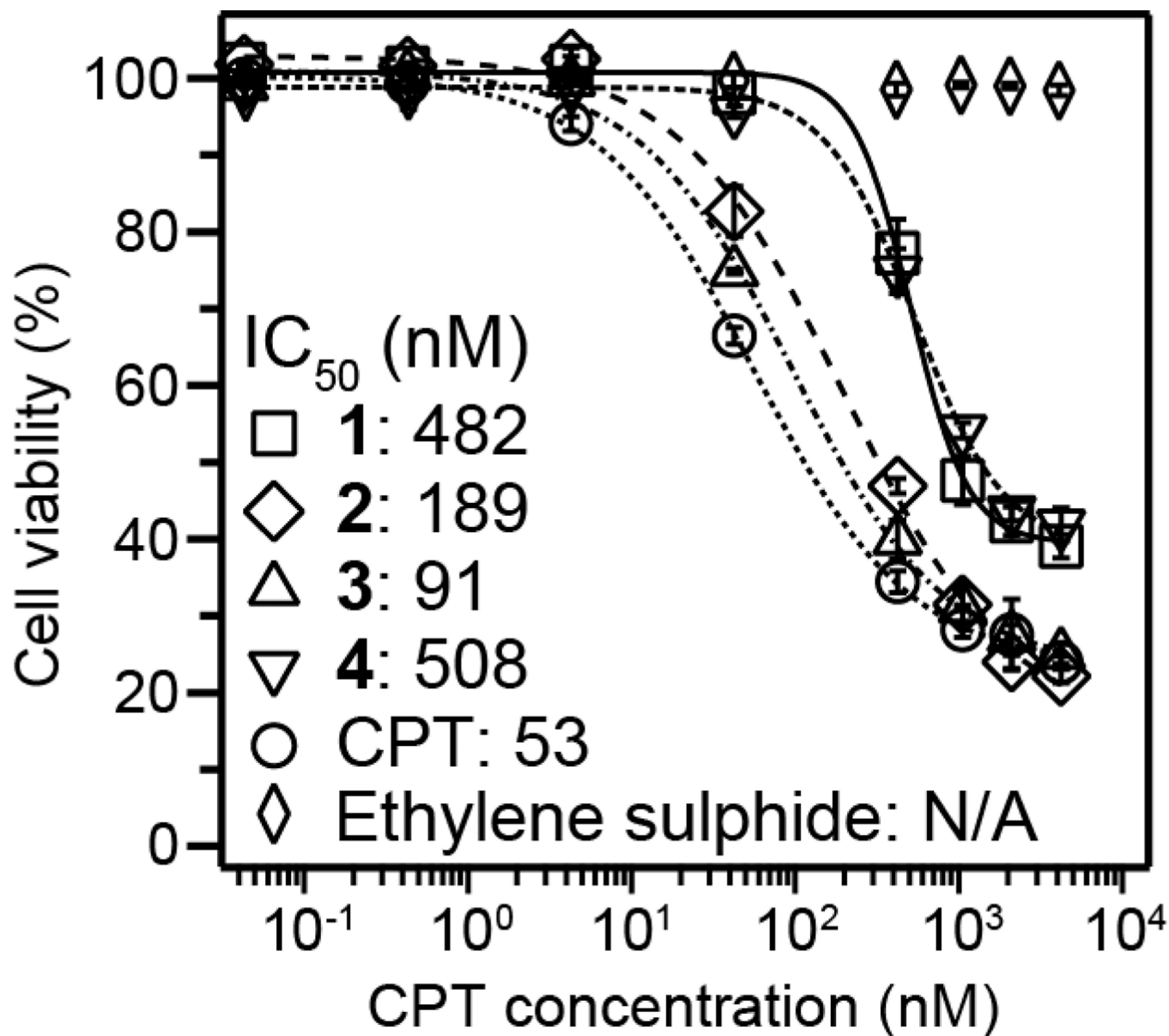


Fig. 4. Cytotoxicity study (48 h incubation) comparing free CPT, **1**, **2**, **3**, **4** and ethylene sulphide against the MCF-7 breast cancer cell line. Cell viability was determined by SRB assay and data are presented as mean \pm s.d. ($n = 3$).